The Journal of Engine Research
Winter 2025, Vol. 71, No. 4, pp. 77-101
Journal Homepage: www.engineresearch.ir

Original Research

Development of a zero-dimensional turbulence model for the flow field of spark-ignition engines, considering vortex motions, based on a new approach

Amir Hosseini Ansaroudi[1], Rahim Khoshbakhti Saray[1,2*], Jafar Pashaei[1]

[1] Faculty of Mechanical Engineering, Sahand University of Technology, Tabriz, Iran
[2] Vehicle Research Institute, Sahand University of Technology, Tabriz, Iran

ARTICLE INFO

Keywords:
Turbulence Model
Zero-Dimensional Model
Tumble Vortex
Turbulence Kinetic Energy
Spark Ignition Engine

ABSTRACT

In this paper, a novel zero-dimensional (0-D) in-cylinder turbulence model has been developed to account for vortex motions in spark-ignition (SI) engines. The flow's mean kinetic energy is decomposed into two distinct components: directional and non-directional flows. To enhance the physical integrity of the model, a directional production term is introduced based on the principles of in-cylinder rotational energy and angular momentum. The traditional production term associated with tumble kinetic energy is replaced by a non-directional production term. It is postulated that the production of turbulent kinetic energy can be linked to the loss of rotational energy through this directional production term, encompassing the energy changes in vortices when the valves are closed and the angular momentum of intake flow when the valves are open. Additionally, the mass flow rate within the cylinder is derived through a one-dimensional (1-D) isentropic flow analysis. To validate the model, experimental investigations are conducted on a natural gas-fueled SI engine, which serves as a reference for model development. The developed model demonstrates the ability to predict the key characteristics of turbulent flow and accurately reproduce the variation of related parameters when compared to the results obtained from three-dimensional (3-D) simulations. Notably, the model requires only a minimal number of tuning constants that are case-insensitive. Furthermore, the results exhibit a high degree of precision near top dead center (TDC) in the compression stroke across all operational cycles.

* Corresponding author
E-mail address: khoshbakhti@sut.ac.ir (R. Khoshbakhti Saray)

Received 3 April 2025; Accepted 10 May 2025
E-ISSN: 2345-4121/ISSN: 1735-5214

Cite this article: Hosseini Ansaroudi A, Khoshbakhti Saray R, Pashaei J. Development of a zero-dimensional turbulence model for the flow field of spark-ignition engines, considering vortex motions, based on a new approach. The Journal of Engine Research. 2025 Feb 19;71(4):77-101. doi: 10.22034/ER.2025.2057048.1083

1- Introduction

In recent decades, concerns regarding environmental issues and the need for energy conservation have grown significantly. Furthermore, heightened consumer awareness of vehicle fuel consumption has increased the imperative to enhance engine performance [1]. To achieve these improvements, a range of technologies have been introduced [2–4], and engines have been optimized to enhance their operational characteristics [5, 6]. The process of optimizing engine performance and employing these technologies often relies on experiments conducted on engine test benches. However, the complexity of modern engines and the high costs associated with experiments have led researchers to increasingly adopt simulations to model engine flow and combustion.

Various approaches exist for modeling engines for research purposes. While three-dimensional (3-D) engine modeling can provide precise results, its implementation is challenging and time-consuming for complex engines [7]. Recently, zero-dimensional (0-D) simulation has emerged as a viable alternative to experiments for advancing engine design, powertrain control, performance optimization, in-cylinder turbulence modeling, and calibration. Once a 0-D model is properly tuned, it can offer reliable consistency even in the absence of experimental data [8].

The utilization of the 0-D approach for modeling turbulence intensity in the flow field of spark-ignition (SI) engines has maintained its prominence in many compact automobiles, motorcycles, and vehicles. This is due to its quieter operation, cost-effective design, and simpler construction [9]. Numerous 0-D turbulence models can be found in the literature.

For instance, Lee and Filipi [10] enhanced the *K*-*k* combustion model for spark-ignition engines, delineating the energy transfer from mean flow kinetic energy (*K*) to turbulence kinetic energy (*k*). Their results demonstrated that this approach serves as a predictive and robust tool for engine optimization and control development. Richard *et al*. [11] simplified a 3-D combustion model to create a 0-D model for simulating heat exchange, knock, and emissions in SI engines. This model incorporated balance equations for turbulence intensity kinetic energy and dissipation rate, yielding accurate estimations for the knock-limited zone, with an absolute error below 2 CAD for 80% of operating points.

Rivas *et al*. [12] applied and validated a novel 0-D flame/wall interaction sub-model for SI engines. Sjeric *et al*. [13] implemented a single-zone *k*-ε turbulence model within a multi-zone combustion model, resulting in significant improvements in predicting both turbulent kinetic energy and the combustion process, a critical aspect of the engine cycle. Bozza *et al*. [14] developed a refined 0-D turbulence model to predict turbulence energy variations in SI engines. This proposed 0-D model demonstrated accurate estimation of in-cylinder turbulence characteristics without necessitating tuning adjustments for changes in engine speed and valve strategy.

In another study, Bozza *et al*. [15] introduced a novel formulation for turbulent energy production based on the analysis of 3-D data. They validated and discussed the outcomes of refining a 0-D turbulence model to predict turbulent intensity in SI engines. Bellis *et al*. [16] introduced a 0-D phenomenological mean flow and turbulence model within the *K*-*k* model family. This newly developed 0-D phenomenological approach characterizes the energy cascade from total mean flow kinetic energy to total turbulent kinetic energy, accounting for primary production and dissipation terms. While this model exhibits reasonable accuracy in predicting turbulence intensity, it faces challenges in correctly identifying peaks within the mean flow velocity profile. Additionally, the developed 0-D model lacks a physical representation of macro vortex motion as directional flow and relies on the adjustment of tuning factors to predict tumble strength and its impact on turbulence intensity.

Recently, Riccardi *et al*. [17] focused on the improvement of the phenomenological

turbulence model, originally conceived to describe turbulence evolution in tumble-promoting engines. The turbulence model was developed with reference to a SI heavy-duty CNG engine derived from a diesel engine. In this architecture, due to the flat cylinder head, turbulence was also generated by swirl and squish flow motions, in addition to tumble motion. The presented turbulence model was validated against 3D CFD results, demonstrating the ability to properly predict turbulence and swirl/tumble evolution under two different operating conditions, without the need for any case-dependent tuning.

Macian *et al*. [18] developed a zero-dimensional model for the combustion process analysis inside a stratified pre-chamber ignition system. First, a *K*-*k*-*ε* model was developed and calibrated according to three-dimensional simulations in motoring conditions performed in a Computational Fluid Dynamic solver (Converge). Then, a thermodynamic model including the mass exchange between both chambers as well as the heat transfer losses to the walls was used to compute the instantaneous heat release rate in the pre-chamber. Both pieces of information were combined to evaluate the effective flame propagation speed, and also to decouple the effects in terms of laminar flame speed, turbulence-flame interaction, and gas velocity due to expansion effects in the burned products.

Perceau *et al*. [19] developed a zero-dimensional turbulence model for a spark-ignition engine in a Miller cycle. The benefits of this strategy, combined with a variable valve timing (VVT) system, were explored using a new 0D model. This model can take into account the strong changes of in-cylinder turbulence generated by the VVT and their effects on the combustion. Efforts have been made to reduce the model's reliance on external inputs. Therefore, analytical calculations of quantities, such as the flame radius, have been favored.

According to the literature, incorporating turbulence parameters enables zero-dimensional (0D) models to more accurately capture the mixing and combustion processes, particularly in spark-ignition engines, where turbulence has a significant impact on flame propagation speed and heat release rates. By including turbulence intensity and integral length scale, the 0D model establishes a stronger connection to the underlying flow physics, effectively bridging the gap between simplified global models and detailed three-dimensional CFD simulations. Moreover, turbulence-informed 0D models reduce the reliance on empirical tuning when applied across varying engine conditions, thereby enhancing their robustness and adaptability over a wide range of speeds, loads, and geometries.

In this study, the aim is to address these limitations by introducing a novel 0-D model that considers the conservative angular momentum of vortex motions. To achieve this, the flow's mean kinetic energy is divided into two distinct components: directional and non-directional flows. Subsequently, a directional production term is introduced based on the principles of in-cylinder rotational energy and angular momentum concepts. This production term contributes to the directional kinetic energy within the system, enhancing the model's physical accuracy. The traditional production term, including tumble kinetic energy, is replaced by a non-directional production term. To develop and validate the new 0-D model, experimental investigations are conducted on a spark-ignition engine. Simultaneously, a 3-D simulation of the combustion domain is employed as the benchmark to verify the results obtained from the 0-D model.

2- Test engine's operating conditions and configurations

In this research, a spark-ignition (SI) MN440A-45GN engine was investigated as a reference for the development of a 0-D turbulence model. The main characteristics of the engine are presented in Table 1. This engine is designed for industrial applications, runs on natural gas, and features electronic throttle control, adjustable ignition timing, and diaphragm mixer devices.

Table 1 MN440A-45GN engine specifications

Parameter	Value
Number of cylinders	4
Bore × Stroke	100 mm × 127 mm
Compression ratio	9.5:1
Connecting rod length	219 mm
Displacement	3.99 L
Firing order	1-3-4-2
Combustion chamber	Heron
Number of valves per cylinder	2
Breathing system	Natural
Fuel	Natural gas
IVO timing relative to TDC of the intake stroke	710°
IVC timing relative to TDC of the intake stroke	223°
EVO timing relative to TDC of the intake stroke	497°
EVC timing relative to TDC of the intake stroke	25°
Maximum inlet valve lift	10.71 mm
Maximum exhaust valve lift	10.84 mm

The data encompassed various spark timings and engine speeds at full load, with details of the engine's operating conditions provided in Table 2. Table 3 presents the accuracy of the measured parameters of the test engine.

Table 2 Engine operating conditions

Case	Engine RPM	Spark timing	Torque (N.m)	$\dot{m}_{air}$ (kg/hr)	$\dot{m}_{fuel}$ (m^3/hr)
1	1200	19 CADBTDC	218	100	9.8
2	1200	26 CADBTDC	225	100	9.8
3	1500	19 CADBTDC	216	120	11.5
4	1500	26 CADBTDC	220	120	11.5
5	2000	19 CADBTDC	185	154	13.2

Table 3 The accuracy of measured parameters

Measured Parameters	Accuracy
Spark Timing	1 CAD±
Air Flow	1%
Fuel Flow	0.5%
Crank Angle	0.1 CAD
IMEP	0.1 bar

3- Model description

3-1- Development of 3-D Model

In this study, a zero-dimensional (0-D) phenomenological model has been formulated for the prediction of turbulence intensity within a spark-ignition (SI) engine. The validity of the proposed model has been assessed by comparing it to the outcomes of a quasi-dimensional thermodynamic model developed by Pashaei and Khoshbakhti [20]. They analyzed the combustion behavior of natural gas fuel through a three-dimensional (3-D) simulation carried out using commercial software, AVL FIRE. The optimal number of computational mesh cells near top dead center (TDC) was approximately 350,000. The schematic representation of the computational mesh within the combustion chamber is illustrated in Figure 1. It is worth noting that the mesh-independence of results was evaluated by monitoring the combustion chamber pressure across different computational mesh cell counts.

The simulation was conducted using the Coherent Flame Model (CFM), with comprehensive details of this approach available in Ref. [21]. Consequently, crucial parameters employed in the CFM, including combustion, spark, and turbulence model specifications, are presented in Table 4.

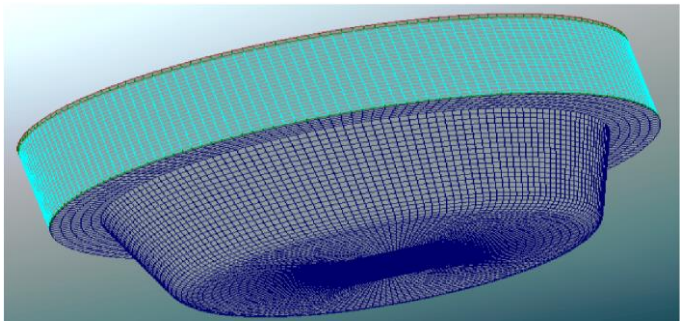

Figure 1 The 3-D model and the schematic diagram of the computational mesh of the combustion chamber

Regarding wall treatment in the simulation, a two-wall treatment approach was employed. Under this approach, the shear stress at the wall is assumed to be a function of turbulent kinetic energy. This assumption helps mitigate the impact of mesh cell size on the overall results [21].

The CFM simulation was performed under closed-valve conditions, and the pressure at the moment of inlet valve closing (PIVC) was derived from experimental data. Additionally, the temperature at this instant, TIVC, was approximated using experimental values of the inlet temperature near the intake port. The initial value of mass-specific turbulent kinetic energy was calculated as:

$k = (3/2) \times (S \times RPM/60)^2$ [34],

where S represents the stroke length. All boundary and initial conditions for the system are outlined in Table 5, with subscripts HW, LW, and PW denoting the head wall, liner wall, and piston wall, respectively.

Table 4 Specifications of the combustion, spark, and turbulence models [34]

Parameter	Specified value
The initial flame surface density	650 1/m
Stretch factor	1.35
Initial flame kernel shape	Spherical
Flame kernel radius	5 mm
Turbulence model	K-e-ζ-f
Wall treatment	Two wall treatment

Table 5 The boundary and initial conditions of the model

Parameter	Value
P_{IVC}	0.97 bar
T_{IVC}	353 K
T_{HW}	600 K
T_{LW}	550 K
T_{PW}	600 K
Mass specific turbulent kinetic energy (MSTKE)	28 m^2/s^2

3-2- Description of the 0-D model

A quasi-dimensional thermodynamic model was developed by the authors based on the concept of the fractal geometry combustion model, focusing on the behavior of natural-gas flames near the combustion chamber walls in SI engines. Specifically, the turbulence characteristics—turbulence intensity and integral length scale—were utilized to calculate both the flame front fractal dimension and characteristic flame wrinkling scale, which are key parameters in the fractal combustion sub-model. These parameters directly influence the burn rate calculation, a core component of the energy release sub-model in the 0-D engine simulation. The burn rate governs the heat release profile and ultimately affects pressure and temperature predictions throughout the cycle. The details of the 0-D model can be found in [20].

3-2-1- Base 0-D Turbulence Model

In this study, the modified energy cascade model developed by Bellis *et al*. [16] serves as the foundational model, having been validated for engines equipped with variable valve actuation systems. The zero-dimensional (0-D) phenomenological approach describes the energy cascade from total mean flow kinetic energy (K) to total turbulent kinetic energy (k), accounting for primary production and dissipation terms. The governing equations for these kinetic energies are expressed as follows [16]:

$$K = \frac{1}{2} m_{cyl} U^2 \tag{1}$$

$$k = \frac{3}{2} m_{cyl} u'^2 \tag{2}$$

$$\frac{dK}{dt} = \dot{K}_{in} - \dot{K}_{ex} + \dot{K}_{tum} - P - D \tag{3}$$

$$\frac{dk}{dt} = \dot{k}_{in} - \dot{k}_{ex} + P - d \tag{4}$$

In Equations (1) and (2), m_{cyl} represents the trapped in-cylinder mass, U denotes the mean flow velocity, and u' represents the turbulent flow velocity. The first term on the right-hand side of both Equations (3) and (4) quantifies the kinetic energy production associated with the intake forward flow and exhaust backflow entering the cylinder, calculated as follows:

$$\dot{K}_{in} = \frac{1}{2} \dot{m}_{in,f} \left(C_{in} u_{in,f}\right)^2 + \frac{1}{2} \dot{m}_{ex,b} \left(C_{ex} u_{ex,b}\right)^2 \tag{5}$$

$$\dot{k}_{in} = \frac{1}{2} \dot{m}_{ex,b} \left(C_{ex} u_{ex,b}\right)^2 \tag{6}$$

In these equations, ṁ represents the mass flow rate, u signifies the isentropic flow speed, and C denotes a tuning constant. The subscripts in, ex, f, and b correspond to intake, exhaust, flow, and backflow, respectively.

The second term on the right-hand side of both Equations (3) and (4) quantifies the kinetic energy associated with the intake backflow and exhaust forward flow exiting the cylinder, calculated as follows:

$$\dot{K}_{ex} = K \frac{\dot{m}_{in,b} + \dot{m}_{ex,f}}{m_{cyl}} \tag{7}$$

$$\dot{k}_{ex} = k \frac{\dot{m}_{in,b} + \dot{m}_{ex,f}}{m_{cyl}} \tag{8}$$

Taking into account the conservative angular momentum of the tumble vortex, Bellis *et al*. [16] illustrated that the term can be expressed in terms of derivatives of density and volume as follows:

$$\dot{K}_{tum} = c_{tum} K \left(\frac{\dot{\rho}}{\rho} - \frac{\dot{V}}{V}\right) \left(w_h \frac{h_{max,PL}}{h_{max,FL}} + (1 - w_h) \frac{\theta_{IVC} - 360}{180}\right) \tag{9}$$

Here, ρ represents density, V signifies volume, c_{tum} denotes the tumble intensity correction term, w_h represents the weight factor, θ_{IVC} represents the intake valve closing angle, and h_{max} stands for the maximum intake valve lift for both part-load (PL) and full-load (FL) scenarios.

The dissipation terms, D and d, in Equations (3) and (4), can be expressed as follows:

$$D = c_D \frac{K}{k} d + 0.5 \frac{\dot{K}_{tum}}{K} \left(1 - \frac{x_p}{S}\right) (2K - k) \tag{10}$$

$$d = 0.09^{0.75} \frac{k^{1.5}}{L_I m_{cyl}^{0.5}} \tag{11}$$

In these equations, c_D, x_p, S, and L_I represent tuning parameters, piston position, stroke, and integral length scale, respectively.

Lastly, the third term on the right-hand side of both Equations (3) and (4), which couples the K and k equations, defines the production term and can be expressed as follows [16]:

$$P = c_P \frac{K}{k} d + 0.5 \frac{\dot{K}_{tum}}{K} \left(1 - \frac{x_p}{S}\right) k \quad (12)$$

The model developed by Bellis *et al*. demonstrates reasonable accuracy in predicting turbulence intensity, but it fails to correctly identify peaks in the mean flow velocity profile. Additionally, the model relies on six tuning parameters (as shown in Equations (1)-(12)), which limits its generalizability across different engine designs and operating conditions. Specifically, these calibrated constants require case-specific adjustment, a process that is both time-consuming and computationally intensive.

A more fundamental limitation is the model's lack of physical representation of macro vortex motion as directional flow. Rather than physically modeling tumble dynamics, it empirically accounts for tumble strength's effect on turbulence intensity through the tuning factor in Equation (9). This approach fails to capture the true physical behavior of tumble vortices, which are inherently directional flows.

To address these limitations—including mean flow velocity prediction inaccuracies, excessive tuning parameters, and insufficient physical basis—this study develops an improved 0-D model. The new formulation enhances physical consistency while maintaining broad applicability.

3-2-2- Proposed 0-D Turbulence Model Concept

To address the concerns highlighted in the preceding section and to account for the tumble macro vortex as directional flow, the mean kinetic energy is partitioned into two distinct kinetic components: directional and non-directional flows [22]:

$$\frac{dK}{dt} = \frac{dK_{non}}{dt} + \frac{dK_{dir}}{dt} \quad (13)$$

Here, K_{non} represents the kinetic energy of non-directional flows, while K_{dir} signifies the kinetic energy associated with directional flows. The kinetic energy of the directional flow is precisely defined by the rotational energy E_{rot}, as articulated in the following equation:

$$\frac{dK_{dir}}{dt} = \frac{dE_{rot}}{dt} \quad (14)$$

Both of the kinetic energies outlined in Equation (13) play roles in the production of turbulent kinetic energy. The contribution of the directional flow to turbulent intensity stems from the alteration in vortex motion, a phenomenon examined by Folga *et al*. [20]. They developed a model to characterize the decay of the tumble vortex during compression and its transformation into turbulence near the top dead center (TDC). By incorporating the K-k approach into their model and considering Equation (13), the governing equation for mean flow kinetic energy can be reformulated as follows:

$$\frac{dK_{non}}{dt} = \dot{K}_{in} - \dot{K}_{ex} - \frac{dK_{dir}}{dt} - P_{non} \quad (15)$$

As previously noted, the term K_{dir} contributes to the production of turbulent intensity and, in accordance with its definition as presented in Eq. (14), encompasses changes in vortex behavior. Consequently, the production term in Eq. (12), which previously included tumble kinetic energy, has been replaced by a non-directional production term, as expressed by [23]:

$$P_{non} = C_\beta \nu_T \frac{2K}{L_g^2} - \frac{2}{3} k \left(\frac{\dot{\rho}}{\rho}\right) - \frac{2}{3} \nu_T \left(\frac{\dot{\rho}}{\rho}\right)^2 \quad (16)$$

In Equation (16), $\nu_T = \frac{0.09 m_{cyl} k^2}{d}$ is based on the standard k-ϵ model, C_β represents a tuning parameter, and L_g is defined as the minimum of (S, 0.5B), with S representing the stroke and B representing the bore of the cylinder. Notably, the terms $\dot{K}_{in}$ and $\dot{K}_{ex}$ in Equation (15) are defined as relations in Equations (5) and (7), respectively. It's worth mentioning that for the tuning parameters in these equations, the relationship $C_{ex} = 0.3C_{in}$ is employed, which is based on findings from previous studies [16, 24].

Furthermore, the mass flow rate in Equations (5) and (7) is determined through a one-dimensional isentropic flow analysis and can be represented as follows [25]:

$$\dot{m} = \begin{cases} \dfrac{C_D A_R P_0}{(RT_0)^{\frac{1}{2}}} \left(\dfrac{P_T}{P_0}\right)^{\frac{1}{\gamma}} \left\{ \dfrac{2\gamma}{\gamma - 1} \left[1 - \left(\dfrac{P_T}{P_0}\right)^{\frac{(\gamma-1)}{\gamma}} \right] \right\}^{\frac{1}{2}} & \dfrac{P_T}{P_0} > \left(\dfrac{2}{\gamma+1}\right)^{\frac{\gamma}{(\gamma-1)}} \\ \dfrac{C_D A_R P_0}{(RT_0)^{\frac{1}{2}}} \gamma^{\frac{1}{2}} \left(\dfrac{2}{\gamma+1}\right)^{\frac{(\gamma+1)}{2(\gamma-1)}} & \dfrac{P_T}{P_0} \leq \left(\dfrac{2}{\gamma+1}\right)^{\frac{\gamma}{(\gamma-1)}} \end{cases} \quad (17)$$

where C_D, P_0, P_T, T_0, and A_R are experimentally determined discharge coefficient, upstream stagnation pressure, flow restriction pressure, upstream stagnation temperature, and reference area, respectively.

For flow entering the cylinder through an intake valve, P_0 represents the intake system pressure, while P_T corresponds to the cylinder pressure. Conversely, for flow exiting the cylinder through an exhaust valve, P_0 represents the cylinder pressure, and P_T represents the exhaust system pressure.

Upon deriving the main equation for mean flow kinetic energy as shown in Eq. (16), the subsequent step is to formulate the governing equation for turbulent kinetic energy. In accordance with the energy cascade model, the transfer of energy from large to small scales results in turbulence production. The presence of friction effects within the cylinder structure causes the dissipation of large-scale kinetic energy into heat. Consequently, variations in turbulence intensity would diminish unless the mean flow of directed charge motion continuously supplies energy [26]. In essence, the rotational energy in each spatial direction, i.e., directional flow kinetic energy, contributes to turbulence production. This production term draws inspiration from a quasi-dimensional model developed by Grasreiner *et al*. [26]. As such, the energy cascade model establishes a connection between the gain in turbulence intensity and the loss of rotational energy. Hence, the directional production term, denoted as P_{dir}, is introduced as follows:

$$\frac{dk}{dt} \propto P_{dir} \propto -\frac{dE_{rot}}{dt} \quad (18)$$

Building upon the concept outlined above and utilizing Eq. (4), the governing equation for turbulent kinetic energy is expressed as follows [19]:

$$\frac{dk}{dt} = P_{dir} - \dot{k}_{ex} + P_{non} - d \quad (19)$$

Equations (18) and (19) highlight that the production of turbulent kinetic energy is intricately linked to the loss of rotational energy through the utilization of a directional production term, which will be further elucidated in the subsequent subsection. Engines may undergo either swirl, tumble, or a combination of these flow patterns within the cylinder, contingent upon the valve train actuation [26]. An appropriate definition for the directional production term will be explored in the upcoming section.

Furthermore, the term "d" in Eq. (19) signifies the dissipation term, as defined in Equation (13). As per this equation, this term is contingent on the integral length scale parameter, L_l, which will be discussed in detail in subsection 5.2.

3-2-2-1- Directional Production Term

In order to determine an appropriate definition for P_{dir}, it is essential to establish a clear understanding of rotational energy, E_{rot}. The definition of rotational energy is provided in references [27, 28], where only non-directional mean flow velocity is considered. More comprehensive definitions are available in the literature, incorporating either tumble or swirl motion [29, 30]. A generalized model based on the global parameter of angular momentum (L) was presented by Grasreiner *et al*. [26], which accounts for both swirl and tumble components.

In this study, the production term is formulated for two operational conditions:

1. Closed-valve conditions, where only shear effects are present
2. Open-valve conditions, which additionally incorporate intake flow energy

Case I: Turbulence in the compression and expansion stroke (closed valves condition)

In this scenario, directional turbulence production, with constant in-cylinder trapped mass, originates solely from the existing rotational energy. Consequently, the term P_{dir} is equivalent to the summation of rotational energies in each direction within the cylinder [22]:

$$P_{dir} = -\sum_{i=xy,z} \frac{dE_{rot,i}}{dt} \tag{20}$$

In this equation, rotational energy is divided into the xy and z directions, which are specified by a right-hand Cartesian coordinate system with the z-axis aligned along the cylinder axis. It is presumed that the primary tumble motion occurs around the x-axis, with minor motion around the y-axis, while swirl motion is envisaged to transpire around the z-axis [31].

The energy term, Erot, is defined with reference to angular momentum L, under the assumption that the flow charge possesses rotational motion [32]:

$$L_i = I_i \omega_i \tag{21}$$

$$E_{rot_i} = \frac{1}{2} I_i \omega_i^2 = \frac{1}{2} \frac{L_i^2}{I_i}, \quad i = xy, z \tag{22}$$

Where I and ω represent the global momentum of inertia and angular velocity, respectively. Assuming a quasi-stationary cylinder geometry, one can differentiate Eq. (22) with respect to time to obtain:

$$\frac{dE_{rot,i}}{dt} = \frac{2E_{rot,i}}{L_i} \frac{dL_i}{dt}, \quad i = xy, z \tag{23}$$

As the valves are closed, with no intake or exhaust flow in this scenario, the angular momentum equation only incorporates the vortex change term in the following form [33]:

$$\frac{dL_i}{dt} = \left(\frac{dL_i}{dt}\right)_{vortex\ change} = L_i \Phi_i \sqrt{k}, \quad i = xy, z \tag{24}$$

In the equation above, the terms Φ_{xy} and Φ_z represent the decay functions of tumble and swirl vortices, respectively. These functions describe the variations of the aforementioned vortices with respect to piston position, and their definitions can be found in Refs. [23, 26].

Case II: Turbulence in the intake stroke (open valves condition)

Continuing with the quasi-stationary cylinder geometry assumption introduced in the previous section, Eqs (20) to (23) remain applicable in this case. However, to express the angular momentum equation, the intake flow angular momentum is described in the following form [23]:

$$\frac{dL_i}{dt} = \left(\frac{dL_i}{dt}\right)_{in} = C_i r_i \dot{m}_{in,f} u_{in,f}, \quad i = xy, z \tag{25}$$

Here, C_i and r_i represent the ratios of angular momentum to linear momentum flux and the tumble/swirl vortex radius, respectively. These parameters are defined as follows:

$$C_i = \frac{2T_i}{\dot{m}_{in,f} u_{in,f} B}, \quad i = xy, z \tag{26}$$

$$r_i = \sqrt{\frac{I_i}{m_{cyl}}}, \quad i = xy, z \tag{27}$$

In equation (26), T_i represents the tumble/swirl torque. The primary concept behind expressing the angular momentum equation in the form of equation (25) is that the intake flow initially possesses linear momentum before entering the cylinder. Subsequently, the

flow undergoes a transformation into rotational flow, resulting in the acquisition of angular momentum. It's worth noting that this rotational flow can be decomposed into tumble and swirl directions, represented by xy and z, respectively. The calculation of the tumble/swirl torque, T_i, can be performed through measurements on a flow bench or by using 3-D simulation data. However, Yoshihara *et al*. [34] derived the following relation to describe this torque:

$$T_i = VR_i \frac{\dot{m}_{in,f}^2}{\rho B}, \quad i = xy, z \tag{28}$$

where VR_i is vortex ratio which is defined by

$$VR_i = \frac{C_{r_i} L_i}{\omega m_{cyl} r_i^2}, \quad i = xy, z \tag{29}$$

Here, C_r represents a tuning parameter. By integrating the approach developed by Bellis *et al*. [16] with the directional flow concept described above, a 0-D turbulence model is formulated.

3-2-2-2- Integral Length Scale

As mentioned earlier, the turbulence model results were validated against a reference 3-D model. Beyond the tuning parameters that affect the alignment between the present model and 3-D simulation results, the integral length scale significantly influences the turbulent intensity model. Therefore, accurately characterizing its temporal variation is essential.

The 3-D simulation results reveal that the integral length scale:

- Reaches minimum values near top dead center (TDC)
- Increases continuously during the intake stroke, peaking at the end of mass entry
- Decreases subsequently, attaining its minimum at compression TDC
- Correlates with the instantaneous in-cylinder height above the piston during expansion/exhaust strokes
- Peaks again at expansion bottom dead center (BDC)
- Declines to its minimum at valve overlap TDC

Given the absence of a direct method to derive the integral length scale from 0-D simulations, researchers have proposed various approximations [24]. In this study, we adopt the expression: $0.05\sqrt[3]{V_{cyl}}$, where V_{cyl} denotes the instantaneous cylinder volume.

3-3- Calibration of model constants

Most mathematical models incorporate constant coefficients that require calibration against experimental data. While literature typically provides valid ranges for these coefficients, their determination must preserve model validity without introducing systematic errors.

Table 6 summarizes the constant coefficients used in this thermodynamic model. The calibration procedure follows three sequential steps:

Step 1: Valve Flow Calibration

- Adjust discharge coefficients for intake/exhaust valves
- Ensure agreement between simulated and experimental:
  · Inlet/outlet mass flow rates
  · Mass exchange during valve overlap

Step 2: Turbulence Calibration

- Optimize coefficients for:
  · Initial turbulence intensity estimation
  · Turbulent kinetic energy generation equations
- Validate against CFD results at:
  · Intake valve closing (IVC) timing
  · Top dead center (TDC)

Step 3: Vortex Dynamics Calibration

- Tune coefficients governing:
  · Vortex ratio formulation
  · Tumble ratio variation prediction

Table 6 Calibration coefficients of the model

Parameter	Symbol	Value
Discharge coefficient of the inlet and outlet valve	Cd_{in}-Cd_{ex}	Variable for different values of valve lift
The constant coefficient for estimating the intensity of the initial turbulence for CFD Simulation	C_m	0.5
Constant coefficient of the turbulent kinetic energy generation equation	C_β	0.38
Constant coefficient of vortex ratio	C_r	0.72

To leverage the benefits of the 0-D phenomenological model, along with the equations mentioned above, it becomes necessary to solve the turbulent flow differential equations concurrently. To achieve this, the mathematical model is solved using a Fortran code. The DVODE solver has been integrated to handle the ordinary differential equations at each crank angle degree (CAD). The simplified flow diagram of the calculation process is illustrated in Figure 2. A comprehensive explanation of the calculation procedure and the resulting outcomes will be provided in the following section.

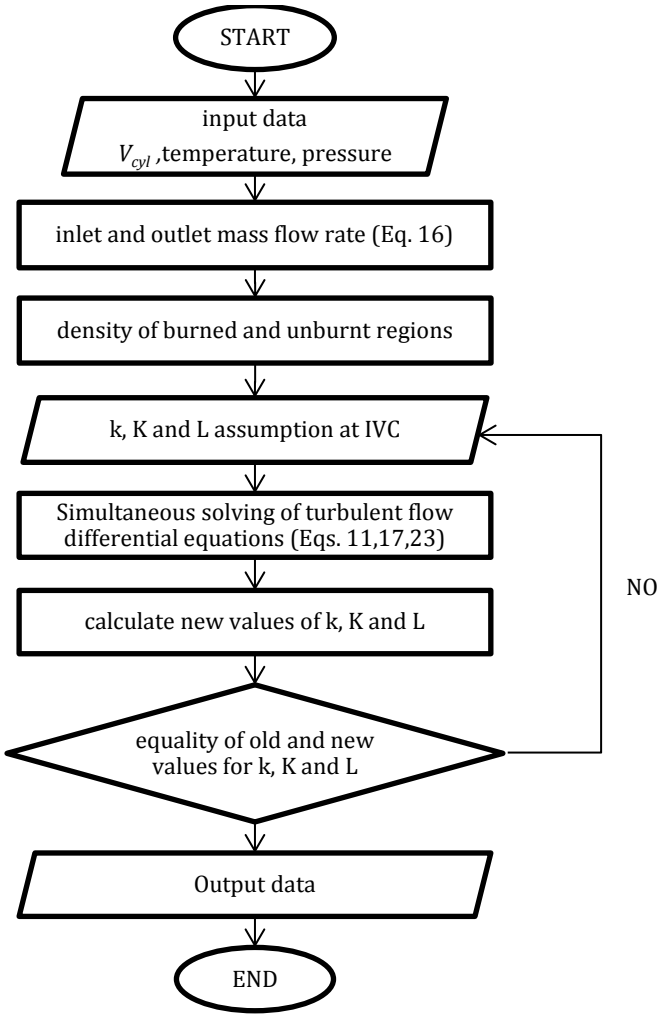

Figure 2 The simplified flow diagram of the calculation

4- Results and Discussion

In this section, the results of the 0-D phenomenological model simulations will be presented and discussed under two conditions: closed and open valves. In the former condition, turbulence intensity is solely influenced by the shear forces of the piston. In the latter condition, when the valves are open, the intake valve flow angular momentum must also be considered. It's important to note that during combustion in the cylinder, the combustion chamber is divided into two regions: burned and unburned. Accordingly, all the parameters within the model are considered with respect to the average mass of each region. After combustion, the entire burned area is represented as a single-zone model in the 0-D approach.

Following the simulation of turbulence intensity in the closed valve condition, the results of simulating the gas exchange process are investigated, taking into account input and output mass flows. Furthermore, as described in the previous section, the effects of tumble and swirl motions are delved into.

Prior to analyzing the results, we outline the model tuning procedure employed in this study. Three key parameters C_{in}, C_{β}, and C_r were calibrated through parametric sensitivity analysis to ensure physically consistent turbulent kinetic energy behavior.

Model validation involved comparing the turbulent kinetic energy predictions from our 0-D model against 3-D simulation results. Figures 3–5 show this parameter's evolution from inlet valve closing (IVC) to exhaust valve opening (EVO) at various engine speeds. Key observations:

- The 0-D model accurately reproduces the 3-D results during compression/expansion strokes
- This agreement is particularly critical for combustion modeling, as turbulence intensity directly affects flame propagation

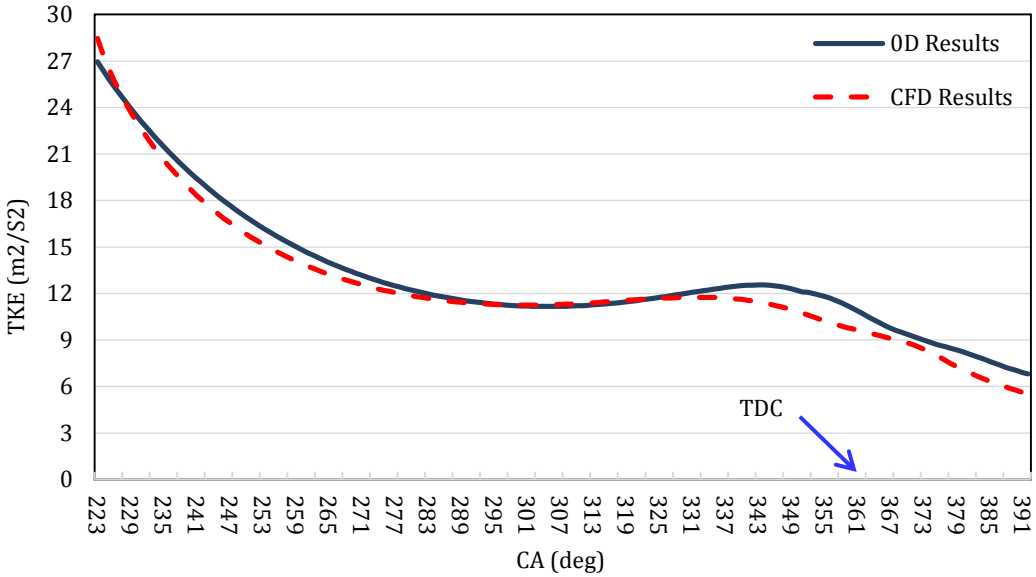

Figure 3 Comparison of the variation of turbulent kinetic energy obtained from 0-D and 3-D models during closed cycle for an engine speed of 1200 rpm and spark timing of 19 CADBTDC

4-1- Validation Scope

Due to the complexity of 3-D modeling for cylinder flow dynamics (non-isentropic behavior, valve-driven effects), comparisons were restricted to closed-valve conditions. However, Section X provides a summary of 0-D model performance during gas exchange.

Following mass entry into the cylinder and inlet valve closure, the turbulence intensity initially peaks due to high flow velocities. However, viscous dissipation progressively

degrades both macro- and micro-scale vortex structures, leading to decreasing turbulence intensity during early compression. As compression progresses, the amplification of tumble and swirl vortices through volume reduction converts rotational energy into turbulent kinetic energy, resulting in a temporary increase (Figures 3–5).

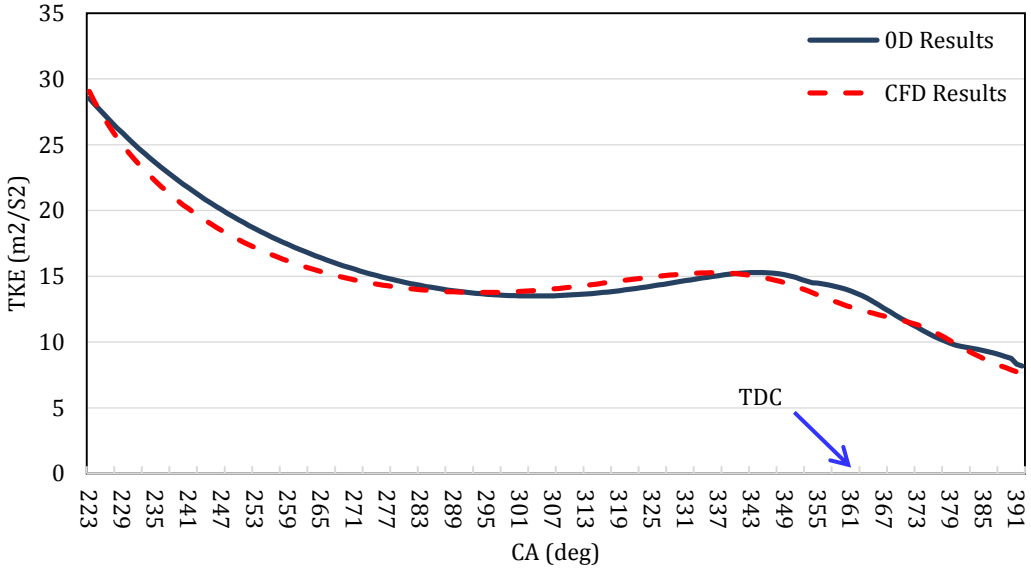

Figure 4 Comparison of the variation of turbulent kinetic energy obtained from 0-D and 3-D models during closed cycle for an engine speed of 1500 rpm and spark timing of 19 CADBTDC

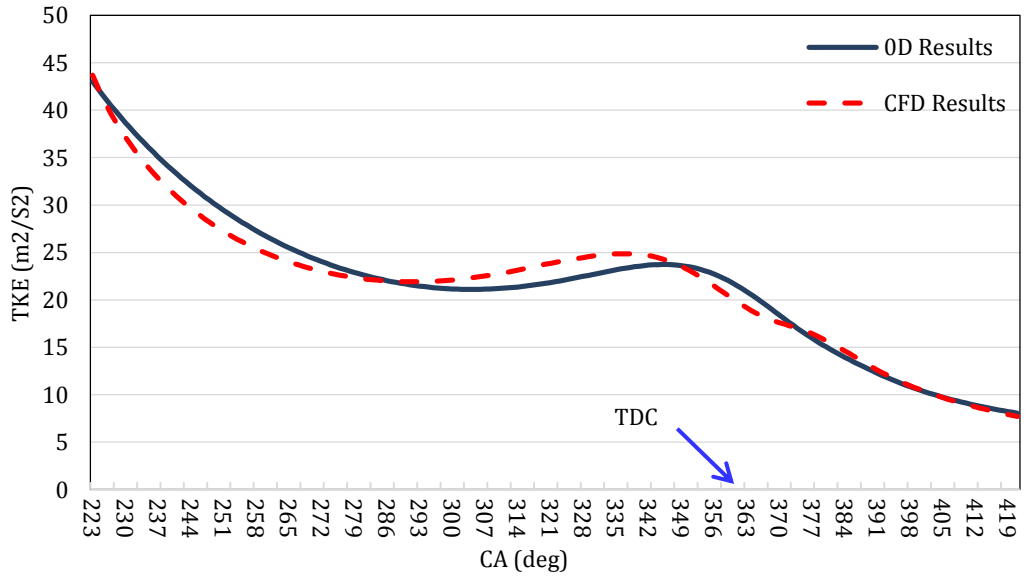

Figure 5 Comparison of the variation of turbulent kinetic energy obtained from 0-D and 3-D models during closed cycle for an engine speed of 2000 rpm and spark timing of 19 CADBTDC

To demonstrate the importance of vortex dynamics in the 0-D model, Fig. 6 compares turbulent kinetic energy predictions with and without directional motion effects, revealing significant discrepancies when vortex changes are neglected.

Figure 6 demonstrates that turbulent kinetic energy in the in-cylinder flow undergoes continuous decay from viscous dissipation regardless of vortex effects, with energy ultimately converting to heat. However, compression-induced amplification of tumble/swirl vortices significantly modifies this parameter's magnitude during this phase.

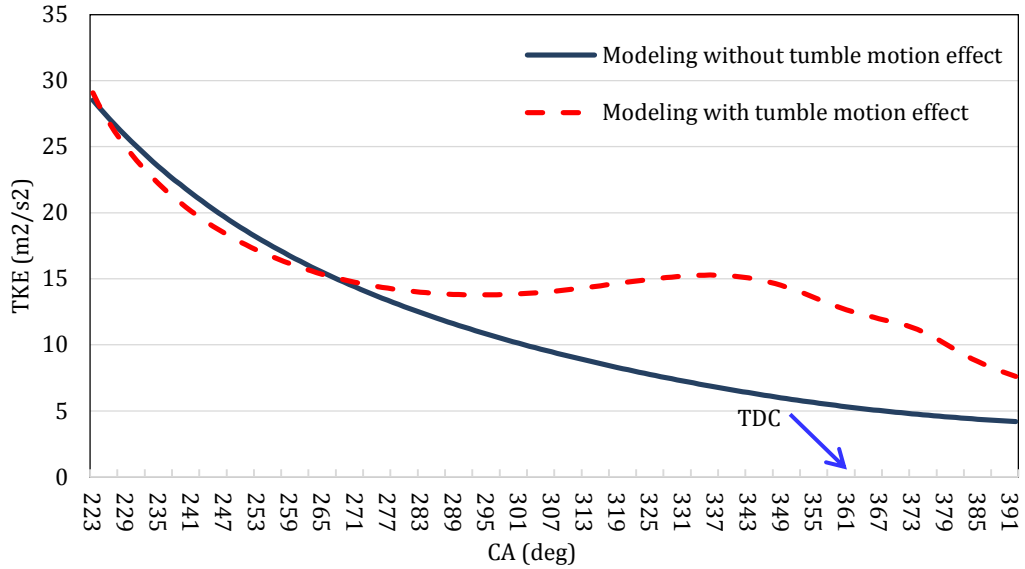

Figure 6 Variation of turbulent kinetic energy obtained from the 0-D model during closed cycle in the presence and absence of vortex change for an engine speed of 1500 rpm and spark timing of 19 CADBTDC

To evaluate the Heron-type combustion chamber geometry (18° declination), Figure 7 presents spatially-resolved turbulent kinetic energy and dissipation rate profiles at multiple piston positions (1500 rpm, spark timing: 19° CA BTDC) from CFD simulations. Key observations:

- Reduced turbulent kinetic energy occurs near piston side/bottom regions due to elevated dissipation rates
- Post-TDC in the power stroke:
  · Dissipation rate increases near piston side walls
  · Turbulent kinetic energy continues rising (combustion-driven generation outpaces dissipation)

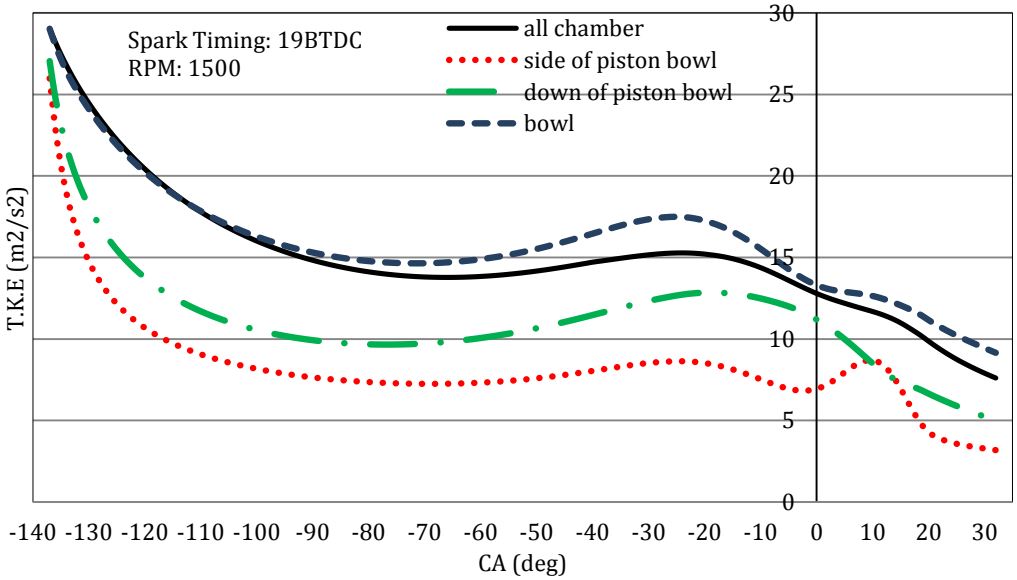

Figure 7 Turbulent kinetic energy variation near the wall versus CA for 1500 rpm and 19 CADBTDC spark timing

This behavior confirms that combustion-induced turbulence generation dominates over dissipation effects near wall boundaries.

Complementing the 3-D simulation validation, a time-step sensitivity analysis was performed to ensure solution independence from temporal resolution. Three crank-angle increments were evaluated:

- 1° CA (baseline)
- 0.5° CA
- 0.3° CA

Figure 8 demonstrates their effects on turbulent kinetic energy evolution:

1. 1° CA resolution:
    - Fails to resolve vortex compression dynamics
    - Underpredicts turbulent kinetic energy by ~15% (peak)
2. 0.5° vs 0.3° CA:
    - Negligible difference (<2%) in results
    - 0.3° CA requires 40% more computational effort

Thus, 0.5° CA was selected as the optimal trade-off between accuracy and efficiency.

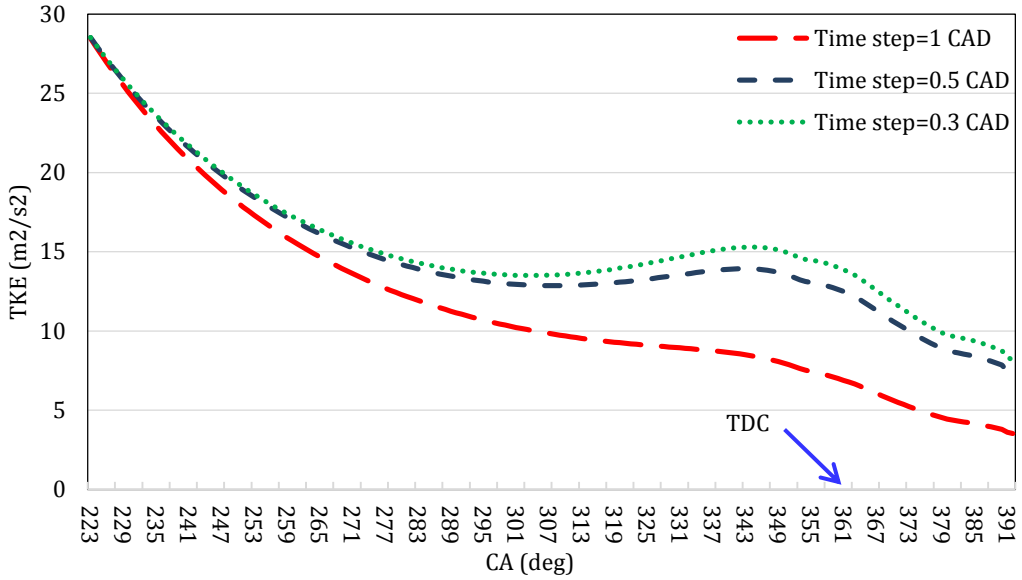

Figure 8 Variation of turbulent kinetic energy for three different crank angle increments in the process of solving equations for an engine speed of 1500 rpm and spark timing of 19 CADBTDC

Following the validation of the results from the 0-D model under the condition of closed valves and the discussion of their independence from the time step, we now turn our attention to examining the influence of engine parameters on the turbulence intensity. Fig. 9 illustrates the impact of engine speed on the variation of turbulent kinetic energy. As depicted in this figure, it becomes evident that as engine speed rises, the flow velocity increases. Consequently, due to the direct correlation between flow velocity and turbulence intensity, turbulent kinetic energy also increases.

The effect of spark timing on turbulent kinetic energy is investigated across various engine speeds. Two distinct spark timing values, 19 CADBTDC and 26 CADBTDC, are considered in the findings. With a spark timing of 26 CADBTDC, the majority of the combustion process occurs during the compression stroke, resulting in higher in-cylinder temperatures and pressures near top dead center compared to those at 19 CADBTDC. These elevated temperatures and pressures lead to a quicker spread of the flame. Consequently, in the case of 26 CADBTDC, there is a slight increase in turbulence intensity.

Figures 10 and 11 display the corresponding 3-D simulation results of turbulent kinetic energy for engine speeds of 1200 rpm and 1500 rpm, respectively. These figures illustrate that spark timing values do not exert a significant influence on turbulent kinetic energy. Thus, it can be concluded that the proposed 0-D model is capable of predicting turbulence intensity across varying spark timing values.

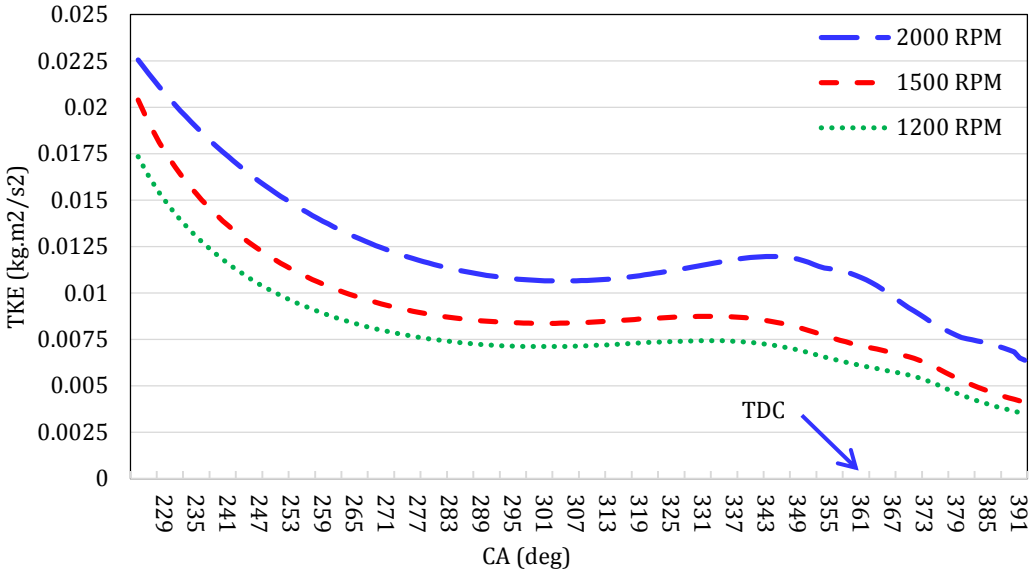

Figure 9 Variation of turbulent kinetic energy obtained from the 0-D model during the closed part of the cycle for different values of engine speed with spark timing of 19 CADBTDC

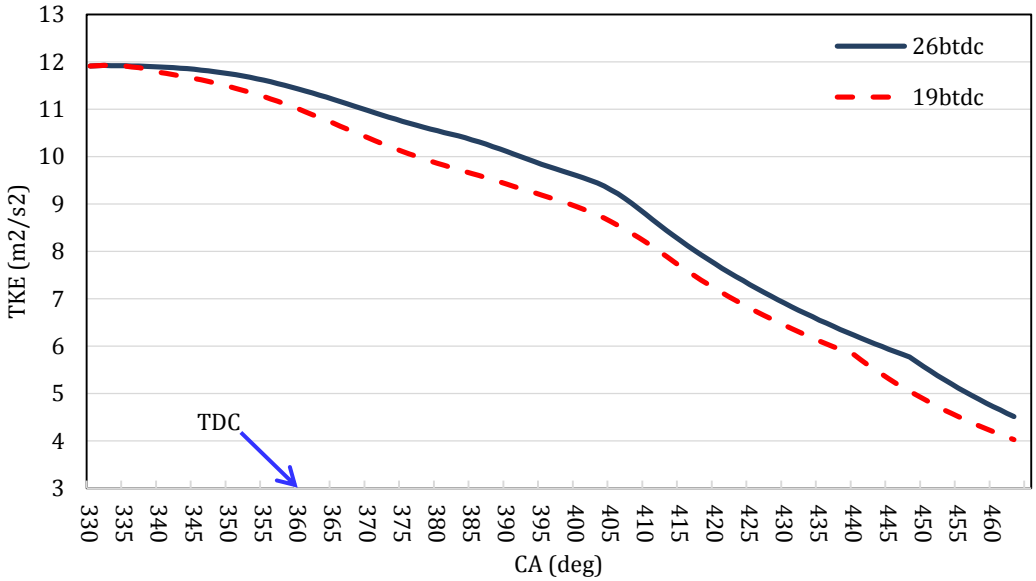

Figure 10 Variation of turbulent kinetic energy based on 3-D simulation for different values of spark timing at an engine speed of 1200 rpm

The investigation focuses on the impact of mass flow rate on turbulent kinetic energy in the context of an open cycle. Mass changes arising from valve opening and closing can be determined using Equation (15). Consequently, Figures 12 and 13 illustrate the time evolution of mass flow rate and in-cylinder mass variation, respectively. Figure 12 demonstrates that when the exhaust valve opens at a crank angle of 497 CAD, combustion products rapidly exit the combustion chamber due to

elevated cylinder pressure, initiating the blowdown process. This trend persists until 565 CAD, after which, as the piston ascends, the exhaust process continues at a reduced rate. During the exhaust phase, valve overlapping occurs with the intake valve opening at 712 CAD. The results reveal that, at this juncture, mass flow rates assume negative values, indicating backflow from both the inlet and exhaust valves. Additionally, in Figure 12, mass variations during this phase are minimal in comparison to the total mass entering and exiting the cylinder. Upon the closing of the exhaust valve at 745 CAD, the fuel and air mixture enters the combustion chamber through the inlet valve. Subsequently, as the piston commences its upward movement from bottom dead center up to 332 CAD, a small fraction of mass escapes through the inlet valve, resulting in a brief period of negative mass flow rate.

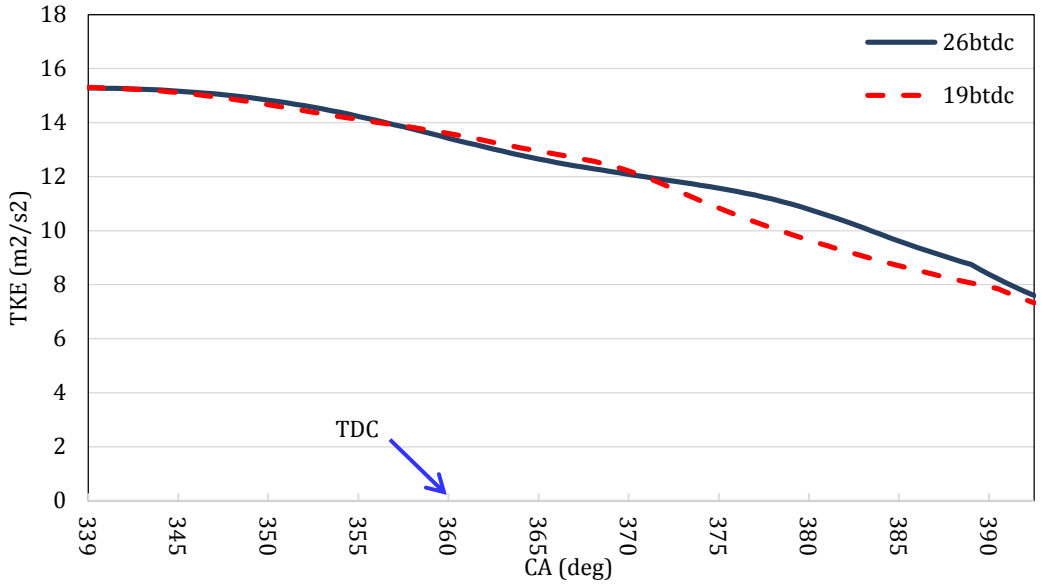

Figure 11 Variation of turbulent kinetic energy based on 3-D simulation for different values of spark timing at an engine speed of 1500 rpm

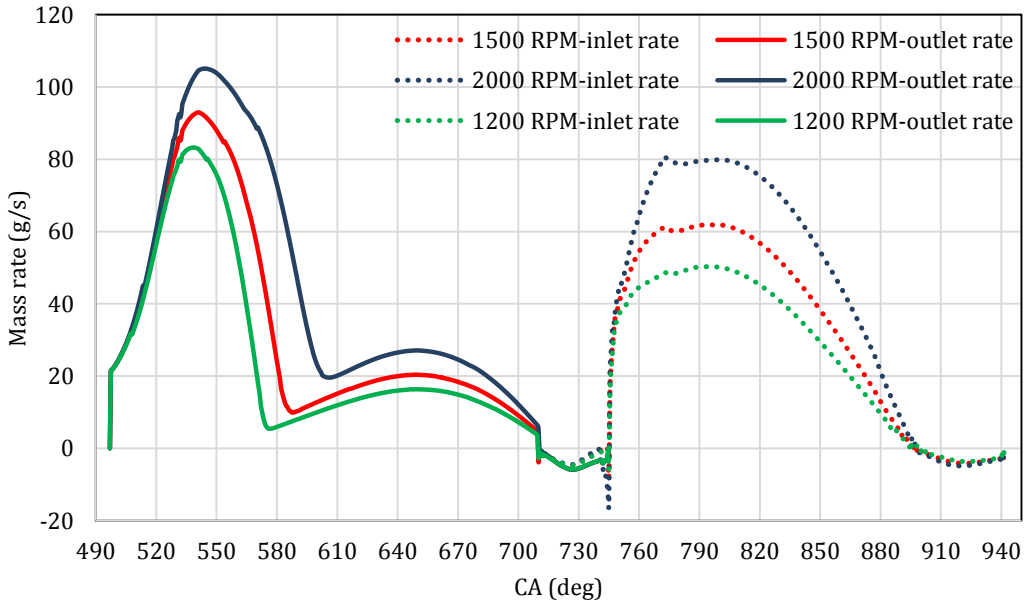

Figure 12 Inlet and Exhaust mass flow rates for engine speeds of 1200 rpm, 1500 rpm and 2000 rpm

Figure 13 illustrates the progression of in-cylinder trapped mass throughout the engine's operational range. Upon comparing the outcomes across three distinct operating speeds, it becomes evident that at higher engine speeds, where the likelihood of mass ingress into the cylinder chamber is reduced, the total trapped mass is also correspondingly diminished. Furthermore, it is noted that at the conclusion of each cycle, the mass content within the cylinder slightly exceeds that of the preceding cycle. This observation signifies the inflow of exhaust mass into the cylinder through the exhaust valve during the overlap period, a phenomenon captured by the simulation of reverse flow.

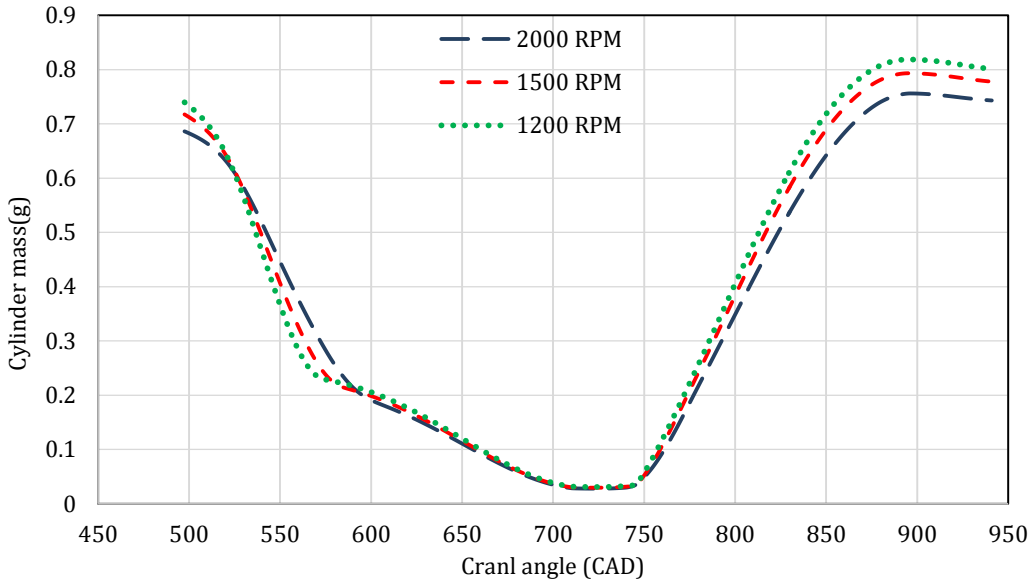

Figure 13 Evolution of trapped in-cylinder mass for three different engine speeds

In Figures 3 to 5, the variation of turbulent kinetic energy for the closed part of the cycle was discussed. Here, by obtaining this parameter for the open part of the cycle, the variation of the total turbulent kinetic energy during the engine operating cycle is shown in Figure 14.

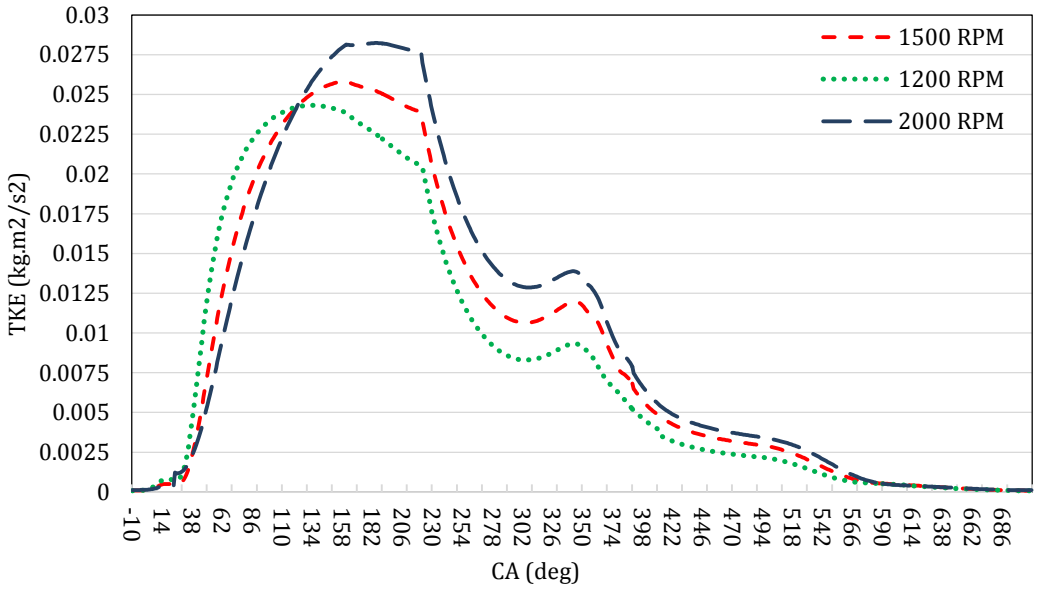

Figure 14 Variation of turbulent kinetic energy obtained from the 0-D model during a complete engine cycle for different engine speeds and spark timing of 19 CADBTDC

Based on the theory outlined in the preceding section, the alterations in the tumble ratio, denoted as VR_{xy}, can be derived using the proposed 0-D model. Figure 15 depicts this parameter across various engine speeds. The characteristics of the tumble vortex can be discerned by examining the variations in the tumble ratio. The vortex formation results from a combination of factors, including the ingress of air through the narrow inlet valve pathway, piston motion, air interaction with the cylinder walls, and the piston's surface. To analyze the behavior of the vortex within the cylinder and its rotational dynamics, distinct phases of tumble ratio variation can be examined as discrete stages. In this study, four such stages have been identified and are illustrated in Figure 16.

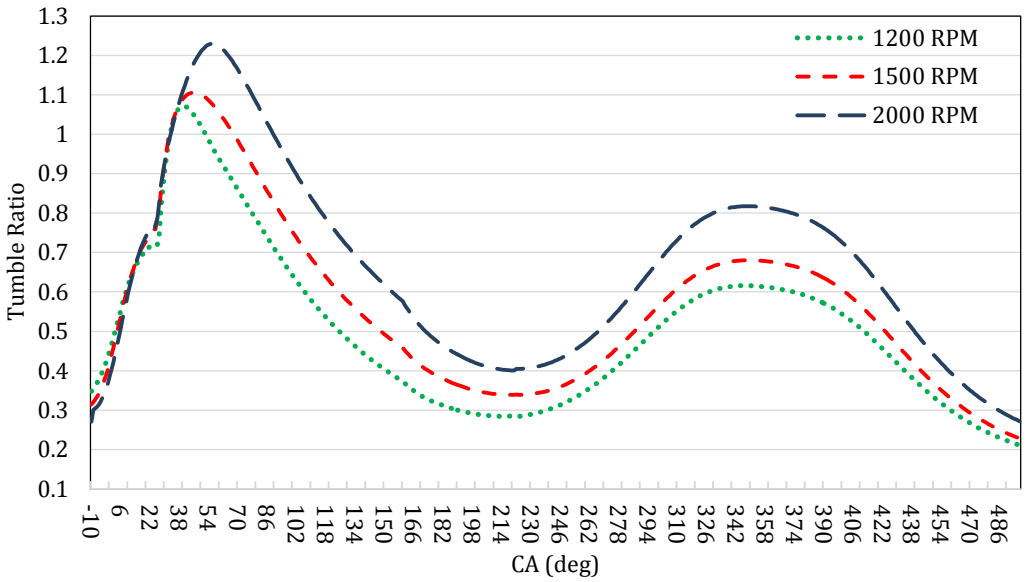

Figure 15 Variation of tumble ratio obtained from a 0-D model for different engine speeds and spark timing of 19 CADBTDC

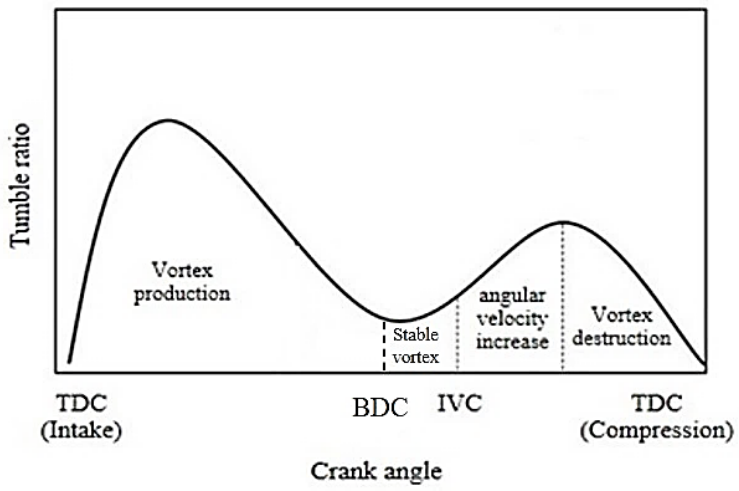

Figure 16 The schematic of the tumble ratio separated into four stages.

As depicted in Figure 16, during the initial stage, the formation of the vortex occurs. This phenomenon is initiated by the entry of air into the cylinder during the intake stroke through the inlet valve, piston movement, airflow against the cylinder walls, and interaction with the piston surface, collectively resulting in the vortex formation.

Moving to the second stage, when the piston reaches bottom dead center of the intake

stroke and just before the valve closes, the rate of vortex dissipation decreases, rendering the vortex relatively stable. However, this stability is transient due to the ongoing energy flow and its eventual dissipation.

Upon the closing of the air valve in the third stage, the tumble vortex encounters compressive forces stemming from the piston's compression action. This compression reduces the size of the vortices, increasing their angular velocity while maintaining constant angular momentum. Consequently, the tumble ratio reaches its peak value during the compression stroke.

Subsequently, in stage four, after the tumble ratio has peaked, the vortex rotates through the piston and the cylinder head, compacting into smaller vortices. This compression process continues as shear forces come into play, leading to the eventual collapse of the tumble vortex around 30 CAD, resulting in a decline in the tumble ratio.

It is important to note that the turbulence characteristics used as input for the zero-dimensional fractal combustion model, namely turbulence intensity and integral length scale, are derived from a three-dimensional CFD simulation that employs the k–ε–ζ–f turbulence model. While this model is widely validated and commonly used for in-cylinder flow simulations, variations in turbulence modeling approaches (such as RNG k–ε, LES, or k–ω SST) could influence the predicted flow structures and turbulence scales. Consequently, the derived parameters used in the 0D model may vary depending on the chosen turbulence model, potentially affecting burn rate predictions and overall combustion performance estimation. Future work may involve performing a comparative study using different turbulence models in the 3D simulation to evaluate the sensitivity of the 0D model's predictions and to further validate the robustness of the proposed approach.

In this study, a single-cycle simulation approach is employed using a zero-dimensional thermodynamic model, and therefore cyclic variations—which arise from changes in residual gas content, turbulence intensity, and combustion timing—are not explicitly considered. These variations can significantly impact combustion stability and performance, particularly at part-load conditions or during transient operation. Incorporating cyclic variability through multi-cycle simulations or stochastic modeling would provide a more comprehensive understanding and is proposed as a direction for future work.

Additionally, manifold pressures at both the intake and exhaust sides are treated as constant boundary conditions for each engine operating point. This simplification enables a focused analysis of in-cylinder turbulence effects. However, in real engine operation, pressure waves and pulsations in the intake and exhaust manifolds can lead to time-dependent pressure fluctuations, especially near valve opening and closing events. These fluctuations can influence mass flow rates and affect in-cylinder pressure and temperature evolution. Including unsteady manifold pressure dynamics in future model extensions could further enhance the predictive capability of the simulation.

5- Conclusions

This study offers a comprehensive description of a zero-dimensional (0-D) phenomenological turbulence model that incorporates vortex motions. The model leverages angular momentum and directional flow concepts to introduce a directional production term, accounting for vortex motions. Calibration of the model was performed against reference experimental data and validated against three-dimensional (3-D) simulation results. The model belongs to the k–k family and elucidates the energy cascade from mean flow to turbulence intensity. It encompasses three tuning constants, with their values derived through sensitivity analysis. This proposed model effectively addresses limitations found in previous models, including inaccuracies in mean flow velocity, excessive tuning factors, and a lack of physical consistency in the vortex model.

The results obtained from the 0-D model exhibit strong agreement with those from the 3-D simulations. The analysis reveals that during the closed phase of the cycle, turbulence intensity initially has a high value, which gradually diminishes due to the influence of viscous forces. Nonetheless, the compression of tumble and swirl vortices, along with their increased rotational energy, engenders additional kinetic energy production within the cylinder, resulting in a temporary surge in turbulent kinetic energy.

The paper also delves into the evolution of turbulent kinetic energy over the entire engine cycle, utilizing tumble ratio variations to probe the effects of vortices on turbulence intensity. This investigation identifies four distinct stages: production, stability, increased vortex angular velocity, and eventual degradation of the tumble vortex.

Nomenclature

Abbreviation

Zero-Dimensional	*0-D*
Three-Dimensional	*3-D*
Air-to-Fuel Ratio	*AFR*
Bottom Dead Center	*BDC*
Crank Angle Degree	*CAD*
Coherent Flame Model	*CFM*
Exhaust Valve Closing	*EVC*
Exhaust Valve Opening	*EVO*
Full-Load	*FL*
Input Valve Closing	*IVC*
Input Valve Opening	*IVO*
Mass Specific Turbulent Kinetic Energy	*MSTKE*
Part-Load	*PL*
Spark Ignition	*SI*
Top Dead Center	*TDC*

Symbols

Reference Area	A_R
Bore	B
Tuning Constant	C
Tuning Parameter	c_D
Discharge Coefficient	C_D
The Ratio of the Angular Momentum to the Linear Momentum Flux	C_i
Tuning Parameter	C_r
Tumble Intensity Correction Term	c_{tum}
Tuning Parameter	C_β
Dissipation Term	D
Dissipation Term Rate	d
Rotational Energy	E_{rot}
Maximum Intake Valve Lift	h_{max}
Global Momentum of Inertia	I
Mean Flow Kinetic Energy	K
Total Turbulent Kinetic Energy	K
The Kinetic Energy of the Directional Flow	K_{dir}
The Kinetic Energy of the Non-Directional Flow	K_{non}
Angular Momentum	L
Integral Length Scale	L_I
Mass Flow Rate	$\dot{m}$
In-Cylinder Mass	m_{cyl}
Production Term	P
Upstream Stagnation Pressure	P_0
Directional Production Term	P_{dir}
Pressure at Inlet Valve Closing Instant	P_{IVC}

Non-Directional Production Term	P_{non}
Flow Restriction Pressure	P_T
Tumble/Swirl Vortex Radius	r_i
Stroke	S
Time	t
Upstream Stagnation Temperature	T_0
Temperature at the Head Wall	T_{HW}
Temperature at Inlet Valve Closing Instant	T_{IVC}
Tumble/Swirl Torque	T_i
Temperature at Liner Wall	T_{LW}
Temperature at Piston Wall	T_{PW}
Mean Flow Velocity	U
Turbulent Flow Velocity	u
Tturbulent Flow Velocity	u'
Volume	V
Instantaneous Cylinder Volume	V_{cyl}
Vortex Ratio	VR_i
Weight Factor	w_h
Piston Position	x_p
Greek Letters	
Density	ρ
Intake Valve Closing Angle	θ_{IVC}
Angular Velocity	ω
Decay Function of Tumble Vortex	Φ_{xy}
Decay Function of Swirl Vortex	Φ_z
Subscripts	
Head Wall	HW
Liner Wall	LW
Piston Wall	PW
Intake	in
Exhaust	ex
Flow	f
Backflow	b
Tumble	tum

References

[1] Kim N, Kim J, Ko I, Choi H, Min K. A study on the refinement of turbulence intensity prediction for the estimation of in-cylinder pressure in a spark-ignited engine. SAE Technical Paper; 2017 Mar 28. doi: 10.4271/2017-01-0525

[2] Scheidt M. Static and transient cylinder deactivation at 4-and 3-cylinder engines. InHyundai-Kia International Powertrain Conference 2015 Oct 27.

[3] Siokos K, Koli R, Prucka R, Schwanke J, Miersch J. Assessment of cooled low pressure EGR in a turbocharged direct injection gasoline engine. SAE International Journal of Engines. 2015 Sep 1;8(4):1535-43.

[4] Kleeberg H, Tomazic D, Dohmen J, Wittek K, Balazs A. Increasing efficiency in gasoline powertrains with a two-stage variable compression ratio (VCR) system. SAE Technical Paper; 2013 Apr 8. doi: 10.4271/2013-01-0288

[5] Lotfan S, Ghiasi RA, Fallah M, Sadeghi MH. ANN-based modeling and reducing dual-fuel engine's challenging emissions by multi-objective evolutionary algorithm NSGA-II. Applied Energy. 2016 Aug 1;175:91-9. doi: 10.1016/j.apenergy.2016.04.099

[6] Bendu H, Deepak BB, Murugan SJ. Multi-objective optimization of ethanol fuelled HCCI engine performance using hybrid GRNN–PSO. Applied Energy. 2017 Feb 1;187:601-11. doi: 10.1016/j.apenergy.2016.11.072

[7] Duclos JP, Zolver M, Baritaud T. 3D modeling of combustion for DI-SI engines. Oil & Gas Science and Technology. 1999 Mar 1;54(2):259-64. doi: 10.2516/ogst:1999023

[8] Won D. A Study on Developing 0-Dimensional Turbulence Model Considering Tumble Motion in a Spark-Ignited Engine. PhD diss., Seoul National University, 2017.
[9] Payri F, Desantes JM, Benajes J. Compression Ignition Engines: State-of-the-Art and Current Technologies. Future Trends and Developments. Handbook of Clean Energy Systems. 2015 Jun 4:1-35. doi: 10.1002/9781118991978.hces079
[10] Lee TK, Filipi ZS. Improving the predictiveness of the quasi-d combustion model for spark ignition engines with flexible intake systems. International Journal of Automotive Technology. 2011 Feb;12:1-9. doi: 10.1007/s12239-011-0001-4
[11] Richard S, Bougrine S, Font G, Lafossas FA, Le Berr F. On the reduction of a 3D CFD combustion model to build a physical 0D model for simulating heat release, knock and pollutants in SI engines. Oil & Gas Science and Technology-Revue de l'IFP. 2009 May 1;64(3):223-42. doi: 10.2516/ogst/2008055
[12] Rivas M, Higelin P, Caillol C, Sename O, Witrant E, Talon V. Validation and application of a new 0d flame/wall interaction sub model for si engines. SAE International Journal of Engines. 2012 Aug 1;5(3):718-33.
[13] Sjeric M, Kozarac D, Bogensperger M. Implementation of a single zone k-ε turbulence model in a multi zone combustion model. SAE Technical Paper; 2012 Apr 16. doi: 10.4271/2012-01-0130
[14] Bozza F, Teodosio L, De Bellis V, Fontanesi S, Iorio A. A refined OD turbulence model to predict tumble and turbulence in SI engines. SAE International Journal of Engines. 2019 Jan 1;12(1):15-30.
[15] Bozza F, Teodosio L, De Bellis V, Fontanesi S, Iorio A. Refinement of a 0D turbulence model to predict tumble and turbulent intensity in SI engines. Part II: model concept, validation and discussion. SAE technical paper. 2018;2018:1-5. doi: 10.4271/2018-01-0856
[16] De Bellis V, Bozza F, Fontanesi S, Severi E, Berni F. Development of a phenomenological turbulence model through a hierarchical 1D/3D approach applied to a VVA turbocharged engine. SAE International Journal of Engines. 2016 Apr 1;9(1):506-19.
[17] Riccardi M, De Bellis V, Sforza L, Beatrice C, Bozza F, Mirzaeian M. Advanced turbulence and combustion modeling for the study of a swirl-assisted natural gas spark-ignition heavy-duty engine. International Journal of Engine Research. 2023 Aug;24(8):3400-16. doi: 10.1177/14680874221150469
[18] Macián V, Salvador FJ, De La Morena J, Pagano V. Combustion analysis of a stratified pre-chamber ignition system by means of a zero-dimensional turbulence and flame speed model. Combustion and Flame. 2021 Oct 1;232:111526. doi: 10.1016/j.combustflame.2021.111526
[19] Perceau M, Guibert P, Guilain S. Zero-dimensional turbulence modeling of a spark ignition engine in a Miller cycle «Dethrottling» approach using a variable valve timing system. Applied Thermal Engineering. 2021 Nov 25;199:117535. doi: 10.1016/j.applthermaleng.2021.117535
[20] Pashaei J, Saray RK. Development of a quasi-dimensional, fractal-base combustion model for SI engines by simulating flame-wall interaction phenomenon. Fuel. 2019 Jan 15;236:13-29. doi: 10.1016/j.fuel.2018.08.155
[21] Marble FE, Broadwell JE. The coherent flame model for turbulent chemical reactions. West Lafayette, IN, USA: Project Squid Headquarters, Purdue University; 1977 Jan 1.
[22] Kim, N. A Study on Phenomenological Quasi-Dimensional Combustion Modeling of Spark-Ignited Engine. PhD diss., Seoul National University, 2016.
[23] Fogla N, Bybee M, Mirzaeian M, Millo F, Wahiduzzaman S. Development of a Kk-ϵ phenomenological model to predict in-cylinder turbulence. SAE International Journal of Engines. 2017 Apr 1;10(2):562-75.
[24] De Bellis V, Severi E, Fontanesi S, Bozza F. Hierarchical 1D/3D approach for the development of a turbulent combustion model applied to a VVA turbocharged engine. Part I: turbulence model. Energy Procedia. 2014 Jan 1;45:829-38. doi: 10.1016/j.egypro.2014.01.088
[25] Heywood JB. Internal Combustion Engine Fundamentals. New York: McGraw-Hill, 1988.
[26] Grasreiner S, Neumann J, Luttermann C, Wensing M, Hasse C. A quasi-dimensional model of turbulence and global charge motion for spark ignition engines with fully variable valvetrains. International Journal of Engine Research. 2014 Oct;15(7):805-16. doi: 10.1177/1468087414521615
[27] Poulos SG, Heywood JB. The effect of chamber geometry on spark-ignition engine combustion. SAE transactions. 1983 Jan 1:1106-29.

[28] Bozza F, Gimelli A, Merola SS, Vaglieco BM. Validation of a fractal combustion model through flame imaging. SAE transactions. 2005 Jan 1:973-87.
[29] Ramajo DE, Zanotti AL, Nigro NN. Validación de un modelo de tumble y turbulencia para un motor de cuatro válvulas de alto rendimiento. Mecánica Computacional. 2005:1527-42.
[30] Eiglmeier C. Phänomenologische Modellbildung des gasseitigen Wandwärmeüberganges in Dieselmotoren [dissertation]. Munich: Technical University of Munich; 2000.
[31] Ferguson CR, Kirkpatrick AT. Internal combustion engines: applied thermosciences. John Wiley & Sons; 2015 Jul 1.
[32] Halliday D, Resnick R, Walker J. Fundamentals of physics. John Wiley & Sons; 2013 Aug 13.
[33] Ramos JI. Internal Combustion Engine Modeling. New York: Hemisphere, 1989.
[34] Yoshihara Y, Nakata K, Takahashi D, Omura T, Ota A. Development of high tumble intake-port for high thermal efficiency engines. SAE Technical Paper; 2016 Apr 5. doi: 10.4271/2016-01-0692

نشریه علمی تحقیقات موتور
زمستان ۱۴۰۳، جلد ۷۱، شماره ٤، صفحه ۷۷-۱۰۱
تارنمای نشریه: www.engineresearch.ir

مقاله پژوهشی

توسعه یک الگوی آشفتگی صفربعدی در میدان جریان موتورهای اشتعال جرقه‌ای با در نظر گرفتن حرکات گردابه‌ها بر اساس رویکرد جدید

امیر حسینی عنصرودی[۱]، رحیم خوشبختی‌سرای[۱و۲*]، جعفر پاشائی[۱]

[۱] دانشکده مهندسی مکانیک، دانشگاه صنعتی سهند، تبریز، ایران
[۲] پژوهشکده خودرو، دانشگاه صنعتی سهند، تبریز، ایران

اطلاعات مقاله

کلیدواژه‌ها:
الگوی آشفتگی
الگوی صفربعدی
گردابه عمودی
انرژی جنبشی آشفته
موتور اشتعال جرقه‌ای

چکیده

در این مقاله، یک الگوی نوآورانه صفربعدی برای در نظر گرفتن حرکات گردابی در موتورهای اشتعال جرقه‌ای توسعه داده شده است. انرژی جنبشی میانگین جریان به دو مؤلفه متمایز جریان‌های جهت‌دار و بدون‌جهت تجزیه می‌شود. به منظور افزایش سازگاری فیزیکی الگو، عبارت تولید انرژی جنبشی جهت‌دار جریان بر اساس مفاهیم انرژی چرخشی در داخل استوانه و گشتاور زاویه‌ای معرفی می‌شود. عبارت تولید مرسوم مرتبط با انرژی جریان گردابه عمودی بوسیله عبارت تولید انرژی جنبشی بدون جهت جایگزین می‌شود. فرض می‌شود که تولید انرژی جنبشی آشفته می‌تواند به از بین رفتن انرژی چرخشی از طریق این عبارت تولید جهت‌دار مرتبط شود که تغییرات انرژی در گردابه‌ها در زمان بسته بودن دریچه‌ها و گشتاور زاویه‌ای جریان ورودی در زمان باز بودن دریچه‌ها را در بر می‌گیرد. علاوه بر این، نرخ جریان جرمی در داخل استوانه از طریق تجزیه و تحلیل جریان یک بعدی بی‌درروی برگشت‌پذیر بدست می‌آید. طرح با نتایج تحقیقات تجربی یک موتور اشتعال جرقه‌ای با سوخت گاز طبیعی اعتبارسنجی شد. الگوی توسعه‌یافته توانایی پیش‌بینی ویژگی‌های اصلی جریان آشفته را دارد. همچنین، این طرح با دقت بالایی توانایی بازتولید تغییرات متغیرها را نسبت به نتایج به دست آمده از شبیه‌سازی سه‌بعدی دارد. شایان ذکر است که این الگو نیاز به تعداد کمی ثابت تنظیمی دارد که به شرایط کارکردی خاص موتور وابسته نیستند. علاوه بر این، نتایج نمایانگر درجه بالایی از دقت در زمان نقطه مکث بالا در طی تراکم در تمامی شرایط کارکردی موتور است.

* نویسنده مسئول
پست الکترونیکی: khoshbakhti@sut.ac.ir (رحیم خوشبختی‌سرای)

دریافت ۱۴ فروردین ۱۴۰۴؛ پذیرش ۲۰ اردیبهشت ۱۴۰۴
شاپای الکترونیکی: ۴۱۲۱-۲۳۴۵ / شاپای چاپی: ۵۲۱۴-۱۷۳۵

Cite this article: Hosseini Ansaroudi A, Khoshbakhti Saray R, Pashaei J. Development of a zero-dimensional turbulence model for the flow field of spark-ignition engines, considering vortex motions, based on a new approach. The Journal of Engine Research. 2025 Feb 19;71(4):77-101. doi: 10.22034/ER.2025.2057048.1083